Applied Science and Technology Ph.D. Program, North Carolina A&T State University
AST 885

Orographic Precipitating Systems

Dr. Yuh-Lang Lin, ylin@cat.edu; http://mesolab.org
Department of Physics/Department of Energy & Environmental Systems
North Carolina A&T State University
(Ref.: *Mesoscale Dynamics*, Y.-L. Lin, Cambridge, 2007)

Chapter 1. Introduction

1.1 The Need for Studying Orographic Precipitating Systems

Why study Orographic Precipitating Systems?

- Many well-known weather phenomena are directly or indirectly related to dry or moist airflow over mountains and their associated precipitation, which could impact our environment and daily life.

Examples of orographically forced flow:

- Lee Waves

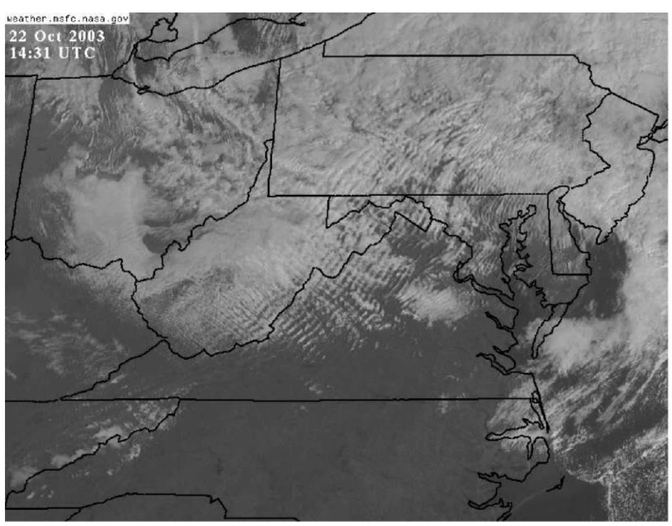

Fig. 5.6: Satellite imagery for lee wave clouds observed at 1431 UTC, 22 October 2003 over western Virginia. Clouds originate at the Appalachian Mountains. (Lin 2007)

- Three-dimensional ship waves formed by airflow over mountainous islands

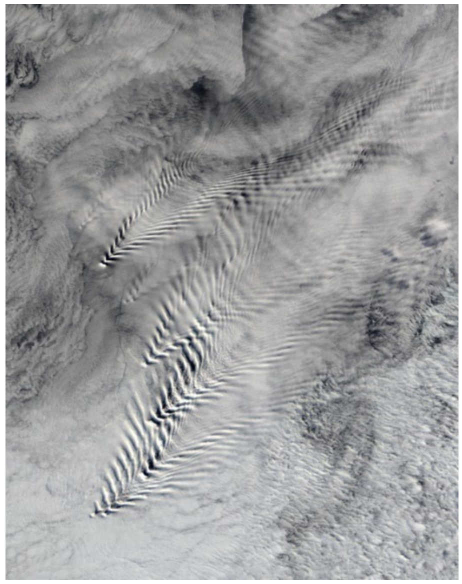

Fig. 5.18: Satellite imagery of trapped three-dimensional lee waves induced by South Sandwich Islands on September 18, 2003. The wave pattern is similar to the ship waves sketched in Fig. 6.19. (From Visible Earth, NASA; Lin 2007)

- Von Karman Vortex Street formed on the lee of a mountainous island (vortex shedding)

Fig. 5.20: Atmospheric vortex street to the lee of the Guadalupe Island revealed by MISR images from June 11, 2000 detected by NASA satellite Terra. This imagery demonstrates

a turbulent atmospheric flow pattern known as von Karman vortex street. (From Visible Earth, NASA; image taken by NASA/GSFC/JPL MISR team) (Lin 2007)

- Severe downslope windstorms

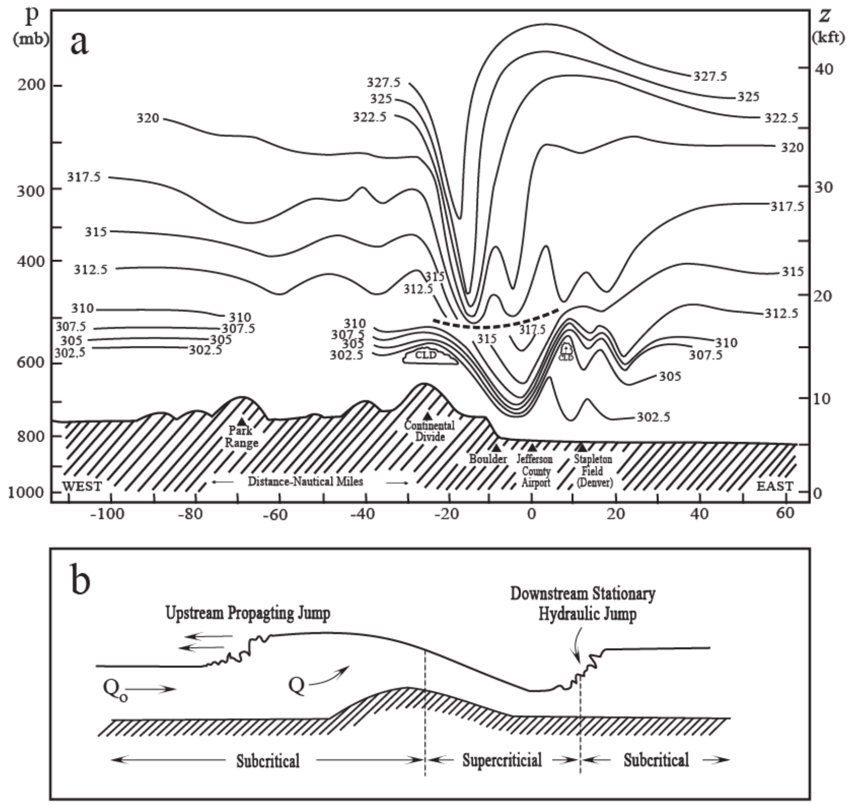

Fig. 3.4: (a) Analysis of potential temperature from aircraft flight data and rawinsondes for the 11 January 1972 Boulder windstorm. The bold dashed line separates data taken from the Queen Air aircraft (before 2200 UTC) and from the Saberliner aircraft (after 0000 UTC) (Adapted after Klemp and Lilly 1975). The severe downslope wind reached a speed greater than 60 ms^{-1}. (b) A sketch of flow Regime C of Fig. 3.3(c), which may be used to explain the phenomenon associated with (a). Q is the volume flux per unit width. (Adapted after Turner 1973; Lin 2007)

- Hydraulic jump on lee side of a mountain

Fig. 3.5: An internal hydraulic jump associated with a severe downslope windstorm formed along the eastern Sierra Nevada (to the right) and Owens Valley, California. The hydraulic jump was made visible by the formation of clouds and by dust raised from the ground in the turbulent flow behind the jump. (Photographed by Robert Symons) (Lin 2007)

- Billow Clouds Formed by Kelvin-Helmholtz Instability

- Orographic Influences on Fronts

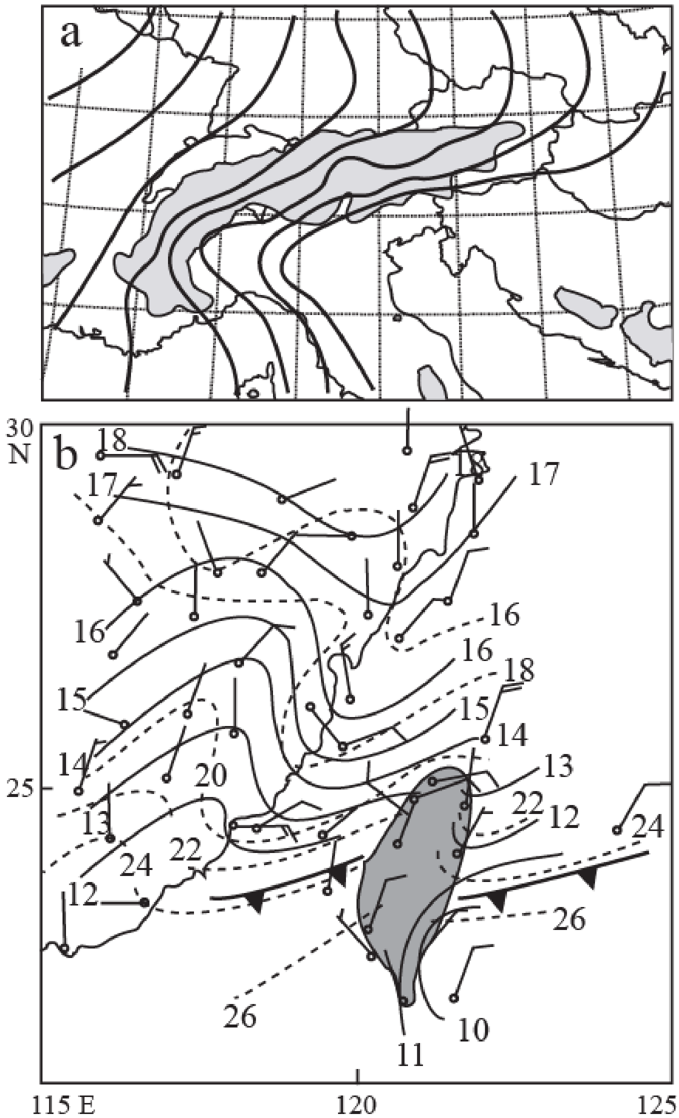

(From Lin 2007)

- Cold-Air Damming by Appalachians

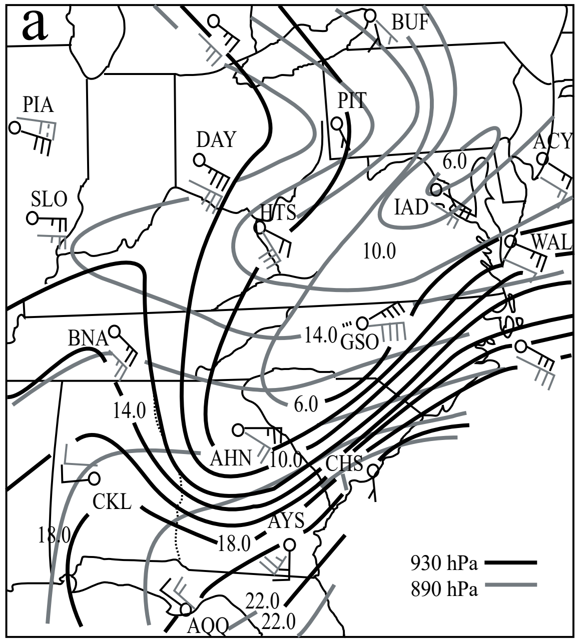

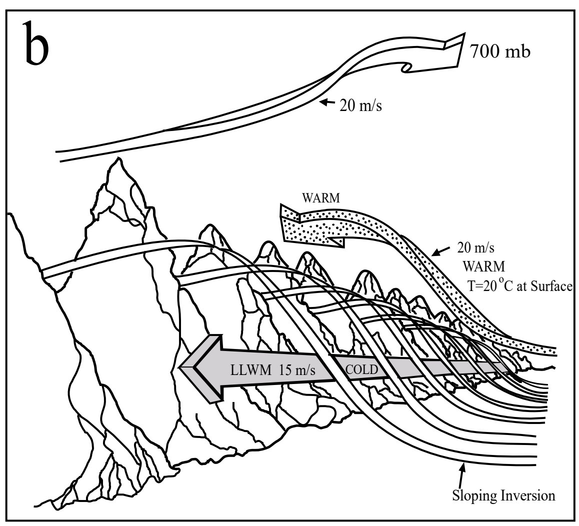

(From Lin 2007)

- Orographic Effects on Cyclones and Cyclogenesis

Lee cyclogenesis over Alps

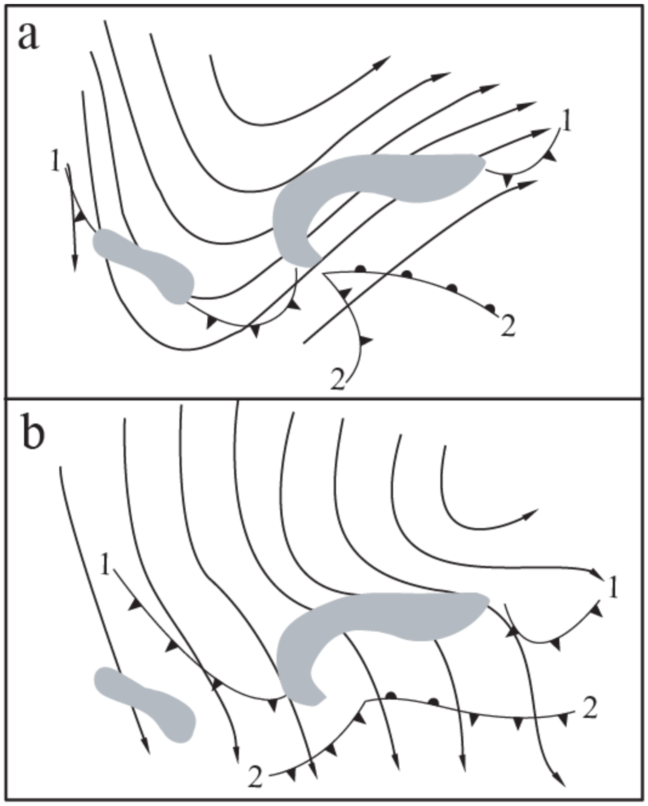

(From Pichler and Steinacker 1987; Lin 2007)

- Orographic Influence on Tropical Cyclone Tracks

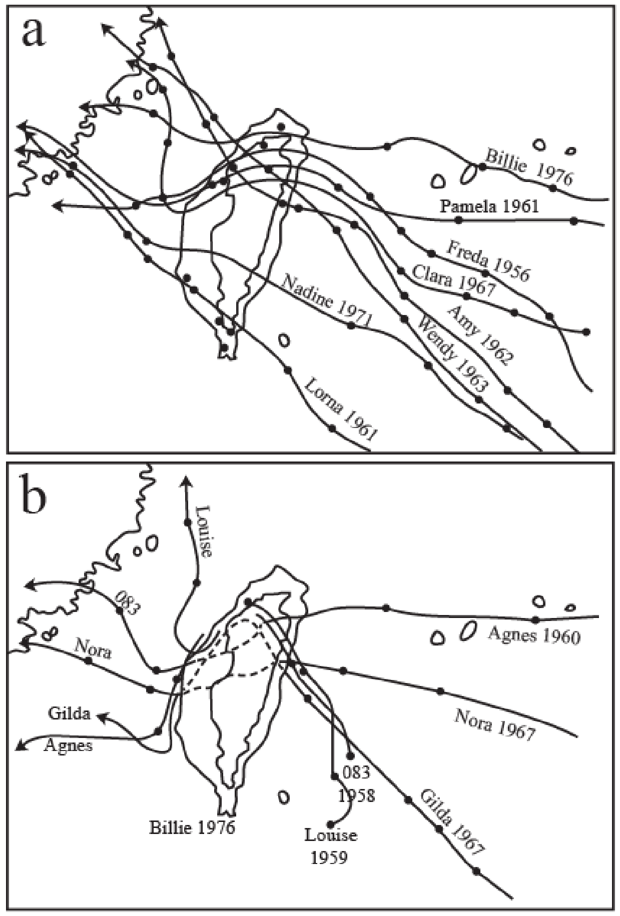

Fig. 5.35: Tropical cyclones traversing the Central Mountain Range (CMR) of Taiwan with (a) continuous tracks, and (b) discontinuous tracks. A cyclone track is defined as discontinuous when the original cyclone (i.e. a low pressure and closed cyclonic circulation) and a lee cyclone simultaneously co-exist. (Adapted after Wang 1980 and Chang 1982) (Lin 2007)

- African Easterly Waves (AEW) originated in E. Africa

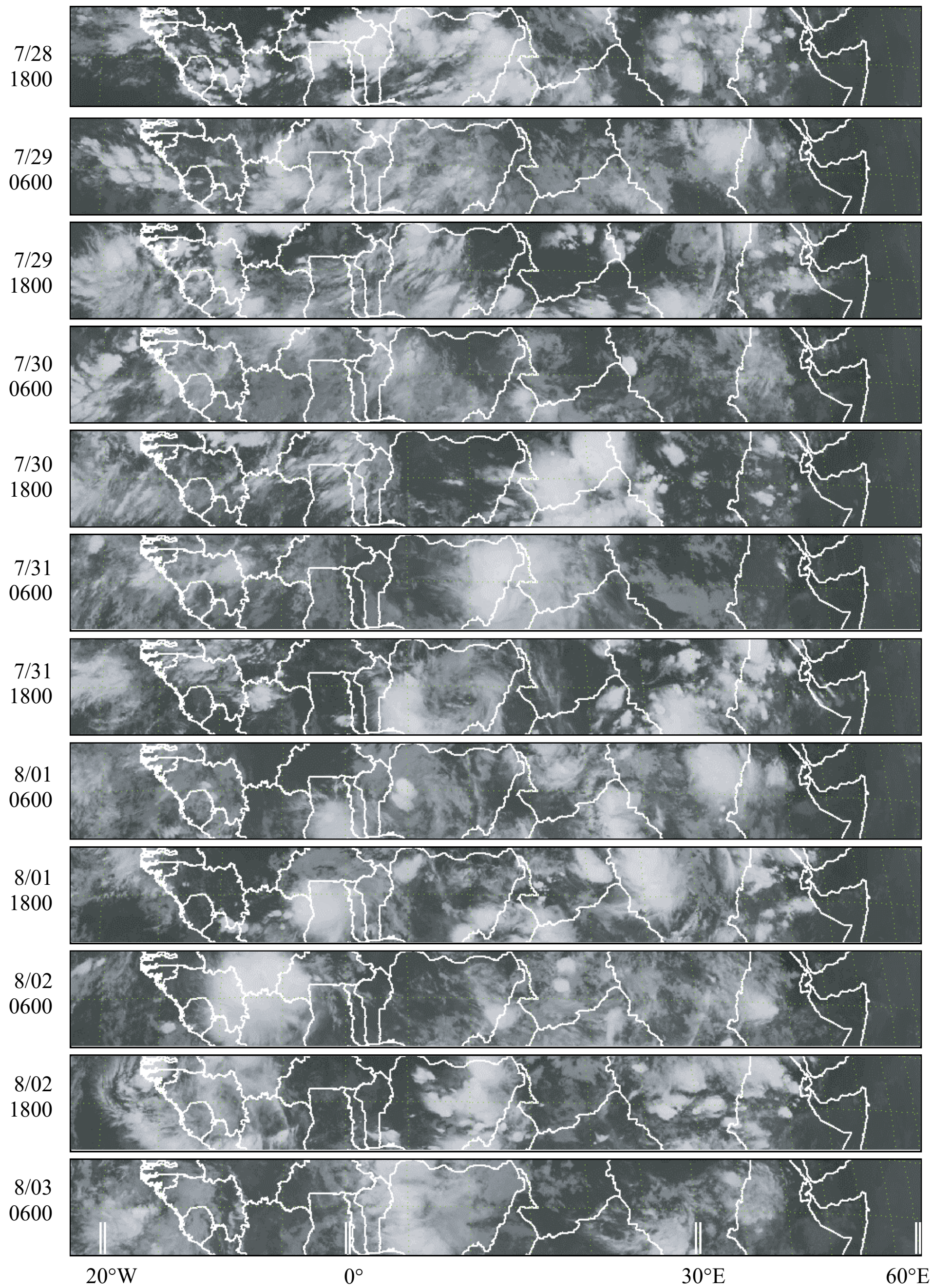

Fig. 9.22: Time-longitude section of METEOSAT-7 infrared satellite imagery for 1800 UTC 28 July 2000 through 1800 UTC 03 August 2000 every 12h. This MCS developed in the lee of the Ethiopian Highlands, was embedded in an African easterly wave and served as a precursor for the tropical depression that developed into Hurricane Alberto over eastern Atlantic Ocean. (From Lin et al. 2005; Imagery from EUMETSAT © 2003) Lin 2007)

- Orographic Influences on large scale flow

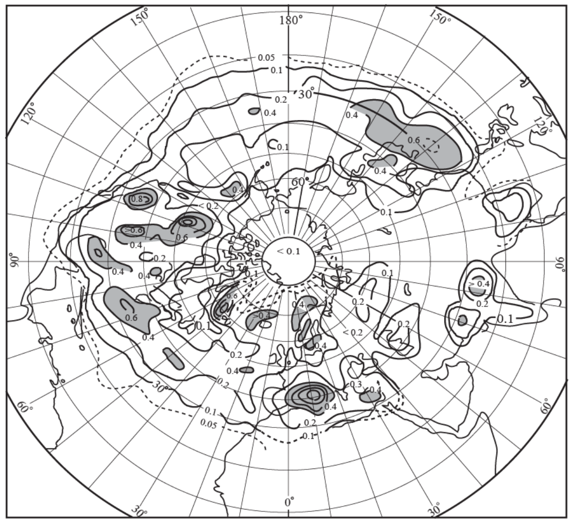

Fig. 5.29: Percentage frequency of cyclogenesis during winter from 1899 to 1939 in the Northern Hemisphere in squares of 100,000 km^2. (Adapted after Petterssen 1956) (Lin 2007)

- Influence on ITCZ

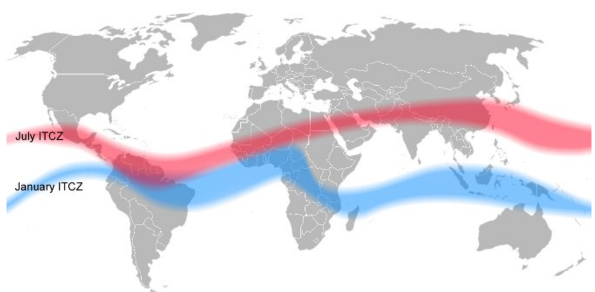

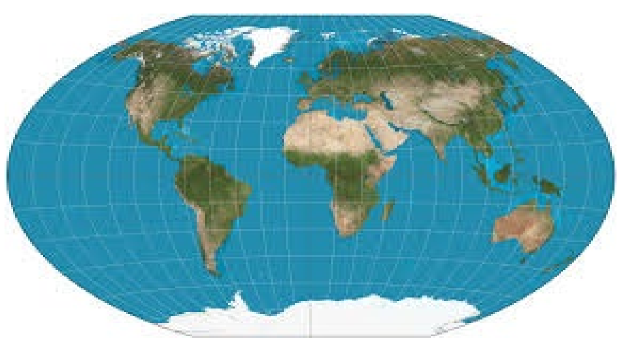

- Orographic Impacts on Storm Tracks

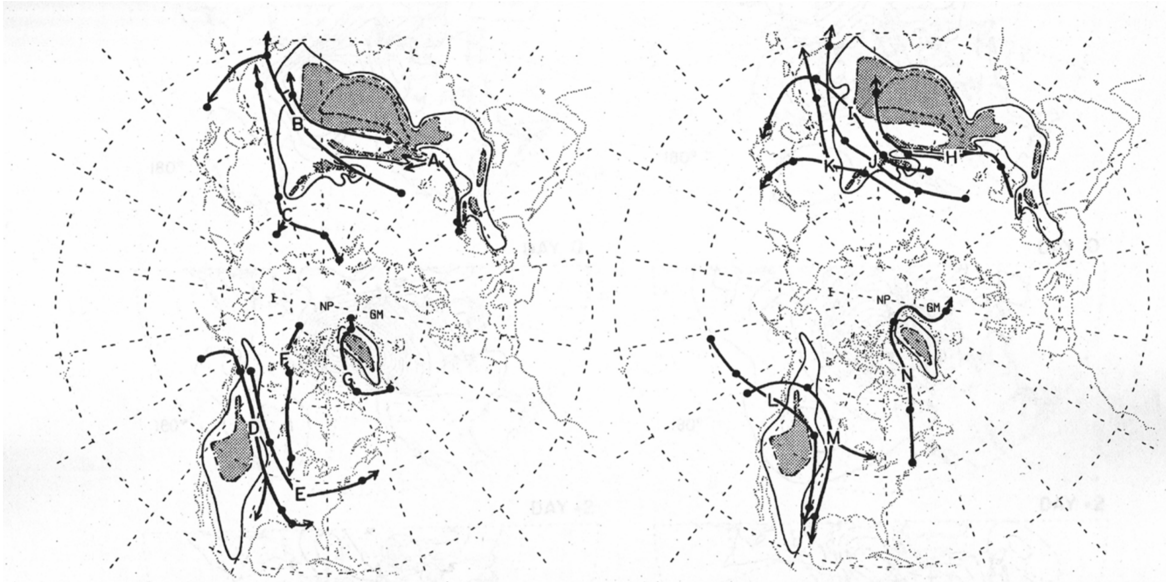

FIG. 15. Paths of phase propagation of unfiltered (left) and high-pass filtered (right) sea-level pressure anomaly patterns based on analysis of lag-correlation maps for many gridpoints. Base gridpoints are marked by letters and centers of the major region of positive correlation in lag-correlation maps with values exceeding 0.2 are marked by dots. Time intervals between dots or between letters and dots are 2 days for the unfiltered anomaly data and one day for the high-pass filtered data. The bifurcation of arrows indicate the distinct propagation paths of splitting correlation patterns. In the region where the propagation is evident and yet no local maxima are indicated by the plotting schemes, no dots are marked and arrow heads indicate the direction of the propagation. Dashed lines are plotted in the region where the propagation is not well-defined. Also sketched are surface elevation contours; solid, dash-dotted and dashed lines correspond to 1, 2 and 5 km, respectively. Areas above 2 km are shaded.

(Hsu 1987 MWR)

Average and Actual Storm Tracks

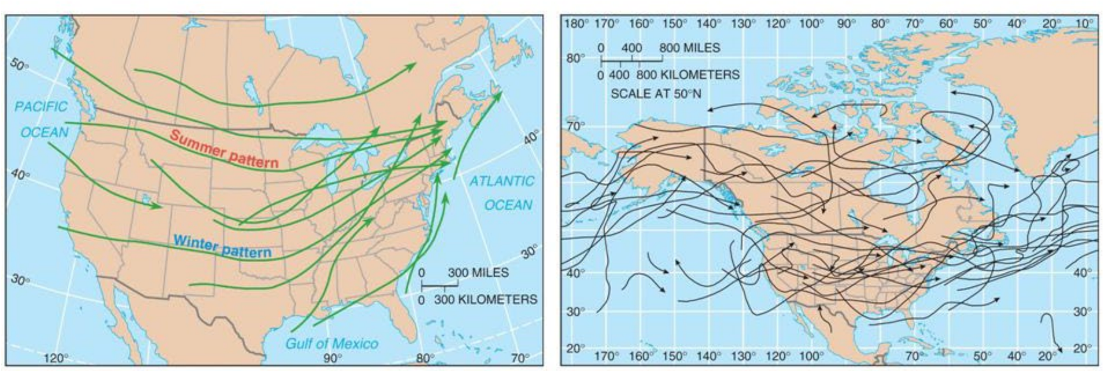

(a) Average storm tracks

(b) Actual storm tracks in March 1991

Figure 8.16 (Link Address)